Atmos. Chem. Phys. Discuss., 11, 23513–23539, 2011
www.atmos-chem-phys-discuss.net/11/23513/2011/
doi:10.5194/acpd-11-23513-2011

Atmospheric Chemistry and Physics Discussions

Discernible rhythm in the spatio/temporal distributions of transatlantic dust

Y. Ben-Ami[1], I. Koren[1], O. Altaratz[1], A. B. Kostinski[2], and Y. Lehahn[1,3]

[1]Department of Environmental Sciences and Energy Research, Weizmann Institute of Science, Rehovot, Israel
[2]Department of Physics, Michigan Technological University, Houghton, Michigan, USA
[3]Department of Geophysics and Planetary Sciences, Tel Aviv University, Tel Aviv, Israel

Received: 27 July 2011 – Accepted: 8 August 2011 – Published: 19 August 2011

Correspondence to: I. Koren (ilan.koren@weizmann.ac.il)

Published by Copernicus Publications on behalf of the European Geosciences Union.

Abstract

The differences in North African dust emission regions and transport routes, between the boreal winter and summer are thoroughly documented. Here we re-examine the spatial and temporal characteristics of dust transport over the tropical and subtropical North Atlantic Ocean, using 10 years of satellite data, in order to determine better the different dust transport periods and their characteristics. We see a robust annual triplet: a discernible rhythm of "transatlantic dust weather".

The proposed annual partition is composed of two heavy loading periods, associated here with a northern-route period and southern-route period, and one clean, light-loading period, accompanied by unusually low average optical depth of dust. The two dusty periods are quite different in character: their duration, transport routes, characteristic aerosol loading and frequency of pronounced dust episodes.

The southern route period lasts about ~4 months, from the end of November to end of March. It is characterized by a relatively steady southern positioning, low frequency of dust events, low background values and high variance in dust loading. The northern-route period lasts ~6.5 months, from the end of March to mid October, and is associated with a steady drift northward of ~0.1 latitude day^{-1}, reaching ~1500 km north of the southern route. The northern period is characterized by higher frequency of dust events, higher (and variable) background and smaller variance in dust loading. It is less episodic than the southern period.

Transitions between the periods are brief. Separation between the southern and northern periods is marked by northward latitudinal shift in dust transport and by moderate reduction in the overall dust loading. The second transition between the northern and southern periods commences with an abrupt reduction in dust loading (thereby initiating the clean period) and rapid shift southward of ~0.2 latitude day^{-1}, and 1300 km in total. These rates of northward advance and southern retreat of the dust transport route are in accordance with the simultaneous shift of the Inter Tropical Front.

ACPD
11, 23513–23539, 2011

Based on cross-correlation analyses, we attribute the observed rhythm to the contrast between the northwestern and southern Saharan dust source spatial distributions. Despite the vast difference in areas, the Bodélé Depression, located in Chad, appears to modulate transatlantic dust patterns about half the time. The proposed partition captures the essence of transatlantic dust climatology and may, therefore, supply a natural temporal framework for dust analysis via models and observations.

1 Introduction

It is well recognized that mineral dust is an essential component in range of processes, involving Earth's radiative budget (e.g.: Highwood et al., 2003; Haywood et al., 2003), generation of clouds and rain (e.g.: Prenni et al., 2009), atmospheric chemistry (Usher et al., 2003 and the references therein), biogeochemical cycles (e.g.: Jickells, et al., 2005), and it has an important impact on human lives (Ozer et al., 2007; Griffin and Kellogg, 2004; Kim et al., 2001). The Atlantic Ocean is the major pathway of dust transport from North Africa, the latter being the Earth largest source of mineral dust (Huneeus, et al. 2011). Therefore, transatlantic dust is of special importance.

North African dust sources are spread over six major regions: (a) over dry lakes in Tunisia and Northern Algeria, (b) along the foothill of the Atlas Mountains and the western coast, (c) along the border between Mali and Algeria, (d) in Central Libya (e) over southern Egypt and Northern Sudan. Regions b and c occupy vast regions over North West Africa. Additional source area is (f) the Bodélé depression, in Chad. It is in a southern position and it is recognized as the vigor dust source in North Africa (Formenti et al., 2010, and the references therein; Koren et al., 2006; Huang et al., 2010).

Dust transport over the Atlantic has been extensively studied, using a variety of sensors, models, and data-sets such as satellite retrievals (e.g.: Karyampudi et al., 1999; Chiapello and Moulin 2002; Torres et al., 2002; Kaufman et al., 2005a; Huang et al., 2010; Sundar and Thomas, 2010), in-situ measurements (e.g.: Reid et al., 2003)

ACPD
11, 23513–23539, 2011

and long records of ground measurements of dust concentration in the western Atlantic (Prospero, 1996, 1999), back-trajectory analysis (Engelstaedter et al., 2009) and transport models (e.g.: Ginoux et al., 2004; Schepanski et al., 2009). These studies recognized a pronounced annual cycle, marked by a latitudinal shift in the transport route over land and ocean and by change in the location of the active dust sources.

Semi-annual "beat" of the Inter Tropical Convergence Zone (ITCZ) that modulates shifts in the prevailing meteorological conditions, the resulting triggering of some of the North African dust sources, and the actual advection of dust, form a complex chain towards transatlantic dust transport. Are there any robust patterns to be expected? To put our questions in proper context, we shall briefly review relevant spatio/temporal patterns discussed in prior literature.

The annual activity of dust sources is correlated with the movement of the synoptic systems. During the boreal summer the northwestern part of Africa is under the influence of a strong heat low, located between the Hoggar and the Atlas (Lavaysse et al., 2009). It aids dust emission as a result of a strong pressure gradient. In this season the border between the northeasterly, dry and hot Harmattan trade winds from the north and the monsoon southwesterly flow of moist and cooler air from the tropical Atlantic (Janicot et al., 2008) creates the Inter Tropical Front (ITF) (Lélé and Lamb, 2010). It is located few hundred kilometers ahead of the ITCZ and supports favored condition for dust emission such as enhanced surface gustiness (Engelstaedter and Washington, 2007) and cold-pool outflow (Bou Karam et al., 2008).

The boreal summer meteorology creates favorable conditions for dust emission mainly from sources located in north-west Africa (Engelstaedter et al., 2006). The Harmattan winds become an important mechanism for emission of dust during the boreal winter. A low level jet, frequently embedded within the Harmattan winds, triggers emission of dust over the Bodélé depression (Washington and Todd, 2005).

Throughout the year, the dust is transported through an east-west corridor over the tropical and subtropical Northern Atlantic. The corridor is generally bounded by the ITCZ in the south, and the westerly winds at mid-low level (located north of ~25°–

ACPD
11, 23513–23539, 2011

30° N), in the north (Sundar et al., 2010). The transport route over the ocean moves along the meridian, in accordance with the shift of the synoptic systems over land.

During the boreal summer, the dust crosses the Saharan coastline and it is transported westward over the ocean by easterly wind, in the Saharan Air Layer (SAL) centered at 700 hPa, above the northeasterly cooler and moister trade winds of the marine boundary layer (Karyampudi et al., 1999; Karyampudi and Carleson, 1988; Prospero and Nees, 1977; Prospero and Carlson, 1972). It is estimated that the SAL is propagated within two consecutive easterly wave troughs. In situ measurements show that the SAL is characterized by frontal characteristics, including gradients in dust concentration, temperature and relative humidity that are pronounced along its leading and southern edges (Reid et al., 2003; Karyampudi et al., 1999). The dust is advected towards the Caribbean Sea and the southern part of North America (Huang et al., 2010). Occasionally the dust is transported via a northern route by the anticyclonic flow over the Azores or Canaries Islands (Karyampudi et al., 1999). It was shown that part of the dust may be transported out of the SAL, by the trade winds at low level above or within the marine boundary layer (Reid et al., 2002; Ben-Ami et al., 2009).

During the boreal winter the dust transport routes shift southward, in accordance with the shift of the synoptic systems and the derived location of the active dust sources. The dust, partly mixed with biomass smoke (Formenti et al., 2008), crosses the coast of West Africa over the Gulf of Guinea (centered at ~4° N) and advected towards the northern part of South America. The dust is transported in lower altitudes than in the summer, below the 700 hPa level (Ben-Ami et al., 2009; Huang et al., 2010). Detailed description of dust transport during the boreal summer months is given in Reid et al. (2003), Karyampudi et al. (1999), Schepanski et al. (2009) and Huang et al. (2010) and during the boreal winter in Kalu (1979), Schepanski et al. (2009) and Huang et al. (2010).

Overall, previous studies approached the North African dust transport over the Atlantic Ocean within the traditional temporal partition of the year, generally the quarterly monthly partition (DJF MAM JJA SON), as markers for changes in dust transport

ACPD
11, 23513–23539, 2011

patterns. The tacit assumption is that temporal variations in dust loading follow the conventional seasonal division. Here we ask whether the conventional seasonal divisions are the best framework to study and describe the annual transatlantic dust route.

In order to answer this question we investigate the spatial and temporal transport patterns of dust loading over the Atlantic Ocean to extract the natural annual cycle of dust over this region and to find improved markers for dust transport periodicity. We then proceed to compare dust emission pattern from the Bodélé depression, known as the most vigorous dust source in the world, to the transatlantic transport patterns in order to interpret the observed differences between the dust periods.

2 Data

The annual cycle of North African dust over the Atlantic Ocean was studied using daily retrievals of total Aerosol Optical Depth (AOD, τ) at 550 nm, obtained from the Moderate Resolution Imaging Spectroradiometer (MODIS) instrument aboard Aqua and Terra satellites. We used Aqua data for the dates between June 2002 and December 2009 and Terra data for April 2000 until December 2009, both in spatial resolution of 1°. All data was taken from collection 5, except the data for 2009, Aqua, when only collection 51 was available. Over ocean the expected error for MODIS retrievals is $\pm 0.03 + 0.05\tau$ (Remer et al., 2008).

The optical depth is a result of extinction of all aerosol types suspended in the atmospheric column. Over the Atlantic Ocean, τ is likely to be the sum of mineral dust, maritime and anthropogenic aerosol from urban and industrial sources and from biomass burning. The expected contribution of anthropogenic aerosol is especially important during the Sahelian biomass burning season (December to February), when the dust transport route passes over the biomass burning region, and the transported dust is mixed with biomass smoke (Formenti et al., 2008). The fraction of τ associated with desert dust (τ_d) is estimated in this work using the following parameters: (a) MODIS retrieval of aerosol fine mode fraction, defined as the fractional contribution of aerosol

ACPD
11, 23513–23539, 2011

with diameter <1 µm to the total τ and attributed to all types of aerosol, (b) estimation of the aerosol fine mode fraction for each one of the three types of aerosol, and (c) estimation of marine aerosol optical depth, based on the wind speed at 1000 hPa, acquired from the National Center for Environmental Prediction (NCEP) reanalysis (Kalnay et al., 1996). Detailed descriptions of the method can be found in Kaufman et al (2005a) and Yu et al. (2009).

Note that this algorithm for extracting τ_d is based on some assumptions regarding the prevalent conditions of dust, maritime and anthropogenic aerosol loading as estimated over specific regions where each type of aerosol is concentrated. τ_d may be either under or over estimated in occasions of high or low dust loading respectively. Additionally, τ_d may be contaminated by the contribution of other type of aerosol, as seen in the Fig. 1 near 10° S and 7° E. Additional source of error in our analysis can be overestimation of τ by ~0.02 due to cloud-contamination (Kaufman et al., 2005b). Nevertheless, by averaging τ over large area and focusing on the low frequencies of the annual cycle of dust, we expect the above errors to be insignificant. Moreover the errors in the dust loading are not expected to affect the recognized spatial pattern of the transport route significantly.

The study area (marked in Fig. 1) was determined based on the spatial distribution of τ_d between the years 2000 and 2009, as shown by the analyzed data, and in accordance with previous studies (e.g.: Kaufman et al., 2005a; Huang et al., 2010). Time series of τ_d were extracted by averaging τ measurements of both MODIS instruments over the study area.

3 Results

Based on analyzing the spatial distribution of dust loading (τ_d), time series of averaged dust loading over the study area and the intra-seasonal loading frequency, we propose that the natural annual cycle of North African dust over the tropical and subtropical North Atlantic Ocean follows three distinct periods and associated spatial patterns.

ACPD
11, 23513–23539, 2011

3.1 Spatial distribution

Figure 2 shows results of spatial analysis using longitudinal and latitudinal Hovmöller diagrams of τ_d over the study area. Two distinct periods of high dust loading are recognized and one clean period when dust loading reduces sharply.

The first dusty period, occurring approximately between the end of November and the end of March, is characterized by southerly transport route that spreads over almost unvarying latitudinal belt, centered around 4° N. During these months, the dust is advected toward the Atlantic Ocean over the northern coast of the Gulf of Guinea and spread between 10° E and 50° W, reaching the northern part of South America. This period will be hereafter denoted as the southern-route period (SRP).

During the second dusty period, occurring approximately between the end of March and mid October, the transport route is characterized by pronounced latitudinal shift in the dust plumes location over the Atlantic of 0.1 latitude day^{-1} (12 km day^{-1}), reaching ~1500 km northwards (Fig. 2a). Over the ocean, the dust spreads between the Saharan coast and 60° W. The center of the dust plume, between ~4° N and 22° N, changes with time. This period will be called the northern-route period (NRP).

The transition from the SRP to the NRP is marked by a latitudinal shift, accompanied by a brief period of reduced τ_d. While the southern route is fixed around latitude 4° N (Fig. 2a), the northern route drifts northward. Between the NRP and SRP there is a clear clean period, characterized by abrupt reduction in the overall oceanic dust loading, shown as vertical and horizontal blue stripes on Fig. 2a, b.

During the clean month period, the whole dust emission setting quickly migrates back south on an average speed of ~0.2 latitude day^{-1} (21 km day^{-1}). The transport route reappears about 1300 km southward, near 4° N, marking the beginning of the SRP and the opening of a new annual cycle. Note that the transition of the transport route from east to west (Fig. 2b) results from the land-ocean geography (for the shape of the coast line see Fig. 1).

ACPD
11, 23513–23539, 2011

3.2 Dust loading

To compliment the information from the Hovmöller diagrams (Fig. 2), in Fig. 3a we display time series of daily τ_d averaged over the study area along with the corresponding low-pass filter curve. The low-pass filter was tuned to the time scale of several weeks, using Daubechie's wavelets (level 6, Daubechies, 1992). The averaged filtered curve (marked in red on Fig. 3a) shows a double peak signal followed by a clear minimum, in agreement with the classification of two dusty periods and one short clean period, as described above. The first annual maximum is attributed to the SRP and the second one to the NRP. The factor of 3 reduction in the value of τ_d, from average of ~0.24, during the maxima of the NRP, to ~0.08, during the minima of the clean period, renders this as a distinct period: the atmosphere over this part of the Atlantic Ocean is substantially less dusty and more transparent.

Extreme episodes are evident (Fig. 3a blue – not filtered data and Fig. 3b) during both dusty periods. These events appear as distinct peaks that are up to 5 times higher than the local average (marked by the red line in Fig. 3). The existence of such spikes, despite the spatial averaging over area of more than 15×10^6 km^2, suggests a coherent emission of dust from many sources throughout North Africa. These massive emissions occur only a few times per year. The unusual weather conditions during these events and part of their climatic impacts were described by Knippertz and Fink (2006), Slingo et al. (2006), Cavazos et al. (2009), Tulet et al. (2008), Thomas and Gautier (2009), and Bou Karam et al. (2010).

Following up on the periodicity gleaned from the time series of τ_d, as shown in Fig. 3 (i.e.: SRP from the end of November until the end of March; NRP between the end of March and mid October), and plotting the daily averaged τ_d vs. the day in the year, major differences between the SRP and the NRP are revealed (Fig. 4a). It is apparent that the SRP is characterized by an almost constant background dust loading of $\tau_d \sim 0.15$. On top of this flat background there are events of very high dust loading with daily average $\tau_d > 0.5$, represented also by the pronounced right tail in the corresponding

ACPD
11, 23513–23539, 2011

histogram of τ_d as shown in Fig. 4b. In contrast, the NRP background dust loading changes through time: It increases from approximately 0.15 at the beginning of the period, to 0.25 at the peak of the period (mid July), followed by a decrease to values of less than 0.1 during the minimum of the clean period (early November). The variance of τ_d during the NRP (0.007) drop by more than an order of magnitude relative to that of SRP (0.01), and suggesting a more continuous flow of dust to the ocean during the NRP.

3.3 Intra-seasonal frequency content

Following the above results we explore the frequency content of the two dusty seasons in more detail. For each period, segments of 60 days around each maximum were concatenated into a single continuous time series throughout the 9 years between 2001 and 2009, keeping the chronological order. The seasonal trends were removed by subtracting the low frequency curve, representing the average annual trend, from the daily data (i.e.: blue curve minus the red curve, Fig. 3a).

Figure 5a shows the two time series, generated for the SRP (left side in blue) and the NRP (right side in red). The frequency content in means of periods of both signals is shown in Fig. 5b. The differences in the patterns of dust loading are clearly evident both on the time series and on the frequency domain. The SRP has pronounced intense and longer-lasting coherent events. This can also be seen from the autocorrelation curves (Fig. 5c): SRP decays more slowly than the NRP and exhibits higher correlations for longer lags.

3.4 What is the role of the Bodélé in the annual cycle of transatlantic dust?

Is there possibly a causal connection between dust emissions from the Bodélé and dust loading over the Atlantic? To that end, we calculated the cross-correlation between the dust loading over the Bodélé (using the deep blue algorithm, Hsu et al., 2004) with the Atlantic one (Fig. 7).

ACPD
11, 23513–23539, 2011

Indeed, Fig. 6a reveals a coherent correlation signal driven by the annual cycle and a clear spike of much higher correlation on a ~3–5 days lag. This is in complete agreement with the average time it takes the dust to travel from the Bodélé over the western coast of Africa and as far as the middle of the Atlantic Ocean (Ben-Ami et al., 2010). Figure 6b, c is for the same signals but with the low-pass seasonal cycle removed.

To further investigate which part of the year contributes to the observed correlation we did the following analysis: a subset of 3 months was extracted from the AOD time series of each of the 10 years. The same duration was extracted for both the Bodélé and the Atlantic data for which a correlation was calculated for a range of time lags. The maximum correlation and the relevant time lag were kept. Next the same analysis was repeated shifting the 3 month sampling range by one day. Such analysis (defined here as running correlation) identifies the parts of the year that contribute the most to the significant synchronicity with the 3 to 5 days lags demonstrated above.

Figure 7 shows that the correlation function maximizes to a value of more than 0.35 during the SRP and minimizes to values of less than 0.1 during the peak of the NRP, when the dust sources location migrates northwards. The time lag for running correlation analysis is between 3 and 5 days for the SRP and 6 to 8 days for the NRP but with much larger variance.

4 Discussion

We showed that dust transport over the Atlantic has an annual triple rhythm composed of two dusty periods followed by a short but distinct clean period. The two dust periods last about 4 and 6.5 months and are different not only in their route location but also in the patterns by which dust is transported over the ocean.

The Southern-route period (SRP) starts around the end of November and ends around the end of March. It is characterized by low levels of background and high variance in dust loading, with coherent and strong events of dust emission that modify

ACPD
11, 23513–23539, 2011

the oceanic dust loading for periods as long as two weeks. The transport route is almost stationary around latitude 4° N, all along the period.

The northern-route period (NRP) is different in all aspects. It starts around end of March and ends around mid October, when Atlantic dust approaches to a minimum loading of less than 0.1 rather fast. Unlike during the SRP, changes in the oceanic dust loading are less episodic. There is a gradual increase in the background dust loading values, reaching its peak around mid July. In contrast to the stationary route pattern of the SRP, the NRP is characterized by a steady migration northward of more than 1500 km in the dust route, between the beginning of the period and its peak. The NRP ends with a short southward movement of the route from 22° N, during the peak of the season, to ~14° N near its end.

During the clean period the average dust loading reduces abruptly to levels of less than 0.1, 2 to 3 times less than the typical loading during the dusty periods. At that time, the whole system continues rests to the southern route of around latitude 4° N. This period lasts about 5–6 weeks.

Figure 8 illustrates schematically the triple beat of the dust loading and the chain saw pattern of dust transport routes over the ocean, the "transatlantic dust weather".

To what extent is this triple beat rhythm linked to the rhythm of emission of the dust sources? Roughly, dust emission can be regarded as a convolution of the source properties and meteorological conditions: Source properties such as mineral content, particle size distribution, vegetation cover, topography and location will determine the potential for available dust. Meteorology governs the triggering of a given source by determining the key environmental factors for dust emission, such as surface winds, humidity and transport winds. The combination will determine how likely this is to be translated into suspended dust flux in the atmosphere.

As a rough approximation, the location of the ITCZ can be a good indicator of the dust meteorology. As stated in the introduction, the synoptic systems that are related to dust emission over North Africa are all moving with the ITCZ. The ITF is located a few hundred kilometers ahead of the ITCZ. The rates we found for the northward advance

ACPD
11, 23513–23539, 2011

of the dust transport route during the beginning of the NRP and the advance southward near its end are in very good agreement with the velocity of the ITF movement at those times of the year (Lélé and Lamb, 2010).

Unlike the NRP that closely follows the ITCZ (and ITF) migration, the SRP stays stationary over latitude 4° N, this can be viewed as a result of the dust sources spatial distribution and their properties (Lélé and Lamb, 2010). While north of the Sahel, all along the western part of the Sahara, there are clusters of many dust sources (Formenti et al., 2010, and the reference therein). Some of which are quite small in area distributing throughout the Western Sahara, the southern sources are bounded by the Sahel that marks the transition from the desert to the savannah. Unlike the northwestern Sahara dust sources, the source distribution on the southern border of the Sahara is sparser, dominated by the world vigorous dust source, the Bodélé depression. In addition, while the sources in north and west Africa (Mali, Mauritania and southern Algeria), are located along the west coast, or up to ~1800 km from the ocean, the Bodélé depression is located about 1800 km from the Gulf of Guinea and between 3000 and 3700 km from the Saharan coast. Such asymmetry between the northern and the southern source distributions can explain many of the presented phenomena of this paper. Many smaller dust sources distribute along the Saharan coast, and closer to the ocean, will emit dust plumes that will follow the location of the maximum surface winds that moves with the ITCZ and the ITF northwards. In contrast, lack of dust sources south of the Sahel will limit transport route to the south. However, the Bodélé depression does supply high dust loading when the surface wind over it exceeds the threshold wind (Koren and Kaufman, 2004). Therefore during the NRP we expect high background dust levels, dominated by high frequencies events marking the contribution of numerous small sources that are closer to the ocean and during the SRP we expect lower frequencies that characterize a single and far, but large source dust emission patterns (the Bodélé).

The cross correlation analysis showed clear synchrony between the Bodélé AOD time series and the Atlantic one. The clear spike in correlation in ~3 to 5 days lag

ACPD
11, 23513–23539, 2011

suggests that the Bodélé is a key source. The detailed running correlation analysis showed that during the SRP the correlations peaked to values of more than 0.4. Such correlation is surprisingly high given the fact that the area around the Bodélé where AOD data was collected (~145 000 km^2) occupies one percent of the Atlantic area in which the AOD is averaged for (~15 $\times 10^6$ km^2).

These results suggest that for the SRP, the Bodélé being the dominant source, serves as a metronome for the Atlantic dust transport that reacts to the Bodélé emission in about 3 to 5 days delay wherein during the NRP the small but denser northern and western Saharan sources dominate. Similar analysis for northwestern Saharan source area shows no significant spikes for the cross correlations and the running correlation analysis peaked to a value of ~0.2 during the NRP.

Acknowledgements. This research was supported in part by the Israel Science Foundation (grant No. 1172\10), and by the Minerva Foundation (grant 780048). Alex B. Kostinski was supported, in part, by NSF AGS.

References

Ben-Ami, Y., Koren, I., Rudich, Y., Artaxo, P., Martin, S. T., and Andreae, M. O.: Transport of North African dust from the Bodérlé depression to the Amazon Basin: a case study, Atmos. Chem. Phys., 10, 7533–7544, doi:10.5194/acp-10-7533-2010, 2010.

Bou Karam, D., Flamant, C., Knippertz, P., Reitebuch, O., Pelon, J., Chong, M., and Dabas, A.: Dust emissions over the Sahel associated with the West African monsoon intertropical discontinuity region: A representative case-study, Q. J. Roy. Meteor. Soc., 134, 621–634. doi:10.1002/qj.244, 2008.

Bou Karam, D., Flamant, C., Cuesta, J., Pelon, J., and Williams, E.: Dust emission and transport associated with a Saharan depression: The February 2007 case, J. Geophys. Res., 115, D00H27, doi:10.1029/2009JD012390, 2010.

Cavazos, C., Todd, M. C., and Schepanski, K.: Numerical model simulation of the Saharan dust event of 6–11 March 2006 using the Regional Climate Model version 3 (RegCM3), J. Geophys. Res. Atmos., 114, D12109, doi:10.1029/2008JD011078, 2009.

ACPD

11, 23513–23539, 2011

Chiapello, I. and Moulin, C.: TOMS and METEOSAT satellite records of the variability of Saharan dust transport over the Atlantic during the last two decades (1979–1997), J. Geophys. Res. Lett., 29, 17–20, doi:10.1029/2001GL013767, 2002.
Daubechies, I.: Ten lectures on wavelets, CBMS-NSF Lecture Notes nr. 61, SIAM, Philadelphia, 1992.
Engelstaedter, S. and Washington, R.: Atmospheric controls on the annual cycle of North African dust, J. Geophys. Res., 112, D03103, doi:10.1029/2006jd007195, 2007.
Engelstaedter, S., Washington, R., and Tegen, I.: North African dust emissions and transport, Earth-Sci. Rev., 79, 73–100, 2006.
Engelstaedter, S., Washington, R., and Mahowald, N.: Impact of changes in atmospheric conditions in modulating summer dust concentration at Barbados: A back-trajectory analysis, J. Geophys. Res., 114, D17111, doi:10.1029/2008JD011180, 2009.
Formenti, P., Rajot, J. L., Desboeufs, K., Caquineau, S., Chevaillier, S., Nava, S., Gaudichet, A., Journet, E., Triquet, S., Alfaro, S., Chiari, M., Haywood, J., Coe, H., Highwood, E.: Regional variability of the composition of mineral dust from western Africa: Results from the AMMA SOP0/DABEX and DODO field campaigns, J. Geophys. Res., 113, D00C13, doi:10.1029/2008JD009903, 2008.
Formenti, P., Schuetz, L., Balkanski, Y., Desboeufs, K., Ebert, M., Kandler, K., Petzold, A., Scheuvens, D., Weinbruch, S., and Zhang, D.: Recent progress in understanding physical and chemical properties of mineral dust, Atmos. Chem. Phys. Discuss., 10, 31187–31251, doi:10.5194/acpd-10-31187-2010, 2010
Ginoux, P., Prospero, J. M., Torres, O., and Chin, M.: Long-term simulation of global dust distribution with the GOCART model: correlation with North Atlantic Oscillation, Environment. Modell. Softw., 19, 113–128, doi:10.1016/S1364-8152(03)00114-2, 2004.
Griffin, D. W. and Kellogg, C. A.: Dust storms and their impact on ocean and human health: dust in Earth's atmosphere, Ecohealth, 1, 248–295, doi:10.1007/s10393-004-0120-8, 2004.
Haywood, J., Francis, P., Osborne, S., Glew, M., Loeb, N., Highwood, E., Tanré, D., Myhre, G., Formenti, P., and Hirst, E.: Radiative properties and direct radiative effect of Saharan dust measured by the C-130 aircraft during SHADE: 1. Solar spectrum, J. Geophys. Res., 108(16), 8577, doi:10.1029/2002JD002687, 2003.
Highwood, E. J., Haywood, J. M., Silverstone, M. D., Newman, S. M., and Taylor, J. P.: Radiative properties and direct effect of Saharan dust measured by the C-130 aircraft during Saharan Dust Experiment (SHADE): 2. Terrestrial spectrum, J. Geophys. Res., 108(13),

ACPD
11, 23513–23539, 2011

8578, doi:10.1029/2002JD002552, 2003.
Hsu, N. C., Tsay, S. C., King, M. D., and Herman, J. R.: Aerosol properties over bright-reflecting source regions, IEEE T. Geosci. Remote, 42, 557–569, 2004.
Huang, J., Zhang, C., and Prospero, J. M.: African dust outbreaks: A satellite perspective of temporal and spatial variability over the tropical Atlantic Ocean, J. Geophys. Res., 115, D05202, doi:10.1029/2009JD012516, 2010.
Huneeus, N., Schulz, M., Balkanski, Y., Griesfeller, J., Prospero, J., Kinne, S., Bauer, S., Boucher, O., Chin, M., Dentener, F., Diehl, T., Easter, R., Fillmore, D., Ghan, S., Ginoux, P., Grini, A., Horowitz, L., Koch, D., Krol, M. C., Landing, W., Liu, X., Mahowald, N., Miller, R., Morcrette, J.-J., Myhre, G., Penner, J., Perlwitz, J., Stier, P., Takemura, T., and Zender, C. S.: Global dust model intercomparison in AeroCom phase I, Atmos. Chem. Phys., 11, 7781–7816, doi:10.5194/acp-11-7781-2011, 2011.
Janicot, S., Thorncroft, C. D., Ali, A., Asencio, N., Berry, G., Bock, O., Bourles, B., Caniaux, G., Chauvin, F., Deme, A., Kergoat, L., Lafore, J.-P., Lavaysse, C., Lebel, T., Marticorena, B., Mounier, F., Nedelec, P., Redelsperger, J.-L., Ravegnani, F., Reeves, C. E., Roca, R., de Rosnay, P., Schlager, H., Sultan, B., Tomasini, M., Ulanovsky, A., and ACMAD forecasters team: Large-scale overview of the summer monsoon over West Africa during the AMMA field experiment in 2006, Ann. Geophys., 26, 2569–2595, doi:10.5194/angeo-26-2569-2008, 2008.
Jickells, T. D., An, Z. S., Andersen, K. K., Baker, A. R., Bergametti, G., Brooks, N., Cao, J. J., Boyd, P. W., Duce, R. A.,. Hunter, K. A, Kawahata, H., Kubilay, N., laRoche, J., Liss, P. S., Mahowald, N., Prospero, J. M., Ridgwell, A. J., Tegen, I., and Torres, R.: Global Iron Connections Between Desert Dust, Ocean Biogeochemistry and Climate, Science, 308, 67–71, doi:10.1126/science.1105959, 2005.
Kalnay, E., Kanamitsu, M., Kistler, R., Collins, W., Deaven, D., Gandin, L., Iredell, M., Saha, S., White, G., Woollen, J., Zhu, Y., Leetmaa, A., Reynolds, R., Chelliah, M., Ebisuzaki,W., Higgins, W., Janowiak, J., Mo, K. C., Ropelewski, C.,Wang, J., Jenne, R., and Joseph, D.: The NCEP/NCAR 40-Year Reanalysis Project, B. Am. Meteorol. Soc., 3, 43–471, 1996.
Kalu, A. E., The African dust plume: Its characteristics and propagation across West Africa in winter, in Saharan Dust: Mobilization, Transport, and Deposition, SCOPE 14, edited by C. Morales, 95–118, John Wiley, New York, USA, 1979.
Karyampudi, V. M. and Carlson, N. T.: Analysis and numerical simulations of the Saharan Air Layer and its effect on easterly wave disturbances, J. Atmos. Sci., 45, 3102–3136, 1988.

ACPD
11, 23513–23539, 2011

Karyampudi, V. M., Palm, S. P., Reagen, J. A., Fang, H., Grant, W. B., Hoff, R. M., Moulin, C., Pierce, H. F., Torres, O., Browell, E. V., and Melfi, S. H.: Validation of the Saharan dust plume conceptual model using lidar, Meteosat and ECMWF, B. Am. Meteorol. Soc., 80, 1045–1075, 1999.

Kaufman, Y. J., Koren, I., Remer, L. A., Tanre, D., Ginoux, P., and Fan, S.: Dust transport and deposition observed from the Terra-Moderate Resolution Imaging Spectroradiometer (MODIS) spacecraft over the Atlantic Ocean, J. Geophys. Res., 110, D10S12, doi:10.1029/2003JD004436, 2005a.

Kaufman, Y. J., Remer, L. A., Tanre, D., Li, R. R., Kleidman, R., Mattoo, S., Levy, R., Eck, T., Holben, B. N., Ichoku, C., Martins, J., and Koren, I.: A critical examination of the residual cloud contamination and diurnal sampling effects on MODIS estimates of aerosol over ocean, IEEE T. Geosci. Remote, 43, 2886–2897, 2005b.

Kim, K. W., Kim, Y. J., and Oh, S. J.: Visibility impairment during Yellow Sand periods in the urban atmosphere of Kwangju, Korea, Atmos. Environ., 35(30), 5157–5167, doi:10.1016/S1352-2310(01)00330-2, 2001.

Knippertz, P. and Fink, A. H.: Synoptic and Dynamic Aspects of an Extreme Springtime Saharan Dust Outbreak, Q. J. Roy. Meteor. Soc., 132, 1153–1177, doi:10.1256/qj.05.109, 2006.

Koren, I. and Kaufman, Y. J.: Direct wind measurements of Saharan dust events from Terra and Aqua satellites, J. Geophys. Res. Lett., 31, L06122, doi:10.1029/2006GL026024, 2004.

Koren, I., Kaufman, Y. J., Washington, R., Todd, C. C., Rudich, Y., Martins, J. V., and Rosenfeld, D.: The Bodélé depression: a single spot in the Sahara that provides most of the mineral dust to the Amazon forest, Environ. Res. Lett., 1, 1–5, 2006.

Lavaysse, C., Flamant, C., Janicot, S., Parker, D. J., Lafore, J. P., Sultan, B., and Pelon, J.: Seasonal evolution of the West African heat low: A climatological perspective, Clim. Dynam., 33, 313–330, doi:10.1007/s00382-009-0553-4, 2009.

Lélé, M. I. and Lamb, P. J.: Variability of the Intertropical Front (ITF) and rainfall over the West African Sudan–Sahel zone, J. Climate, 23, 3984–4004, doi:2010/10.1175JCLI3277.1, 2010.

Ozer, P., Laghdaf, M., Lemine, S. O. M., and Gassani, J.: Estimation of air quality degradation due to Saharan dust at Nouakchott, Mauritania, from horizontal visibility data, Water Air Soil Poll., 178, 79–87, 2007.

Prenni, A. J., Petters, M. D., Kreidenweis, S. M., Heald, C. L., Martin, S. T., Artaxo, P., Garland, R. M., Wollny, A. G., and Pö oschl, U.: Relative roles of biogenic emissions and Saharan dust as ice nuclei in the Amazon Basin, Nat. Geosci., 2, 402–405, 2009.

ACPD

11, 23513–23539, 2011

Prospero, J. M.: The atmospheric transport of particles to the ocean, in Ittekkot V, Schäfer P, Honjo S, and Depetris P J (eds) Particle Flux in the Ocean SCOPE Report 57 John Wiley & Sons Chichester 19–52, 1996.

Prospero, J. M.: Long-term measurements of the transport of African mineral dust to the southeastern United States: Implications for regional air quality, J. Geophys. Res., 104, 15917–15927, 1999.

Prospero, J. M. and Carlson, T. N.: Vertical and areal distribution of Saharan dust over the western equatorial North Atlantic ocean, J. Geophys. Res., 77, 5255–5265, 1972.

Prospero, J. M. and Nees, R. T.: Dust concentration in the atmosphere of the equatorial North Atlantic: Possible relationship to the Sahelian drought, Science, 196, 1196–1198, 1977.

Reid, J. S., Westphal, D., LLivingston, J. M., Savoie, D. L., Maring, H. B., Jonsson, H. H., Eleuterio, D. P., Kinney, J. E., and Reid, E. A.: Dust vertical distribution in the Caribbean during the Puerto Rico Dust Experiment, J. Geophys. Res., 29, 1151, doi.:10.1029/2001GL014092, 2002.

Reid, J. S., Kinney, J. E., Westphal, D. L., Holben, B. N., Welton, E. J., Tsay, S., Eleuterio, D. P., Campbell, J. R., Christopher, S. A., Colarco, P. R., Jonsson, H. H., Livingston, J. M., Maring, H. B., Meier, M. L., Pilewskie, P., Prospero, J. M., Reid, E. A., Remer, L. A., Russell, P. B., Savoie, D. L., Smirnov, A., and Tanré , D.: Analysis of measurements of Saharan dust by airborne and ground-based remote sensing methods during the Puerto Rico Dust Experiment (PRIDE), J. Geophys. Res., 108, D19,8586, doi:10.1029/2002JD002493, 2003.

Remer, L. A., Kleidman, R. G., Levy, R. C., Kaufman, Y. J., Tanre, D., Mattoo, S., Martins, J. V., Ichoku, C., Koren, I., Yu, H. B., and Holben, B. N.: Global aerosol climatology from the MODIS satellite sensors, J. Geophys. Res., 113, D14S07, doi:10.1029/2007JD009661, 2008.

Schepanski, K., Tegen, I., and Macke, A.: Saharan dust transport and deposition towards the tropical northern Atlantic, Atmos. Chem. Phys., 9, 1173–1189, doi:10.5194/acp-9-1173-2009, 2009.

Slingo, A., Ackerman, T. P., Allan, R. P., Kassianov, E. I., McFarlane, S. A., Robinson, G. J., Barnard, J. C., Miller, M. A., Harries, J. E., Russell, J. E., and Dewitte, S.: Observations of the impact of a major Saharan dust storm on the atmospheric radiation balance, J. Geophys. Res., 33, L24817, doi:10.1029/2006GL027869, 2006.

Sundar, A. C. and Thomas, A. J.: Satellite and surface-based remote sensing of Saharan dust aerosols, Remote Sens. Environ., 114, 1002–1007, 2010.

ACPD
11, 23513–23539, 2011

Thomas, M. and Gautier, C.: Investigations of the March 2006 African dust storm using ground-based column-integrated high spectral resolution infrared (8–13 µm) and visible aerosol optical thickness measurements: 2 Mineral aerosol mixture analyses, J. Geophys. Res., 114, D14209, doi:10.1029/2008JD010931, 2009.

Torres, O., Bhartia, P. K., Herman, J. R., Sinyuk, A., Ginoux, P., and Holben, B.: A long-term record of aerosol optical depth from TOMS observations and comparison to AERONET measurements, J. Atmos. Sci., 59, 398–413, 2002.

Tulet, P., Mallet, M., Pont, V., Pelon, J., and Boone A.: The 7–13 March 2006 dust storm over West Africa: Generation, transport, and vertical stratification, J. Geophys. Res., 113(13), D00C08, doi:10.1029/2008JD009871, 2008.

Usher, C. R., Michel, A. E., and Grassian, V. H.: Reactions on mineral dust, Chem. Rev., 103, 4883–4939, 2003.

Washington, R. and Todd, M.C.: Atmospheric controls on mineral dust emission from the Bodélé Depression, Chad: The role of the low level jet, J. Geophys. Res., 32, L17701, doi:10.1029/2005GL023597, 2005.

Yu, H. B., Chin, M., Remer, L. A., Kleidman, R. G., Bellouin, N., Bian, H. S., and Diehl, T.: Variability of marine aerosol fine mode fraction and estimates of anthropogenic aerosol component over cloud-free oceans from the Moderate Resolution Imaging Spectroradiometer (MODIS), J. Geophys. Res., Atmosphere, 114, D10206, doi:10.1029/2008JD010648, 2009.

ACPD
11, 23513–23539, 2011

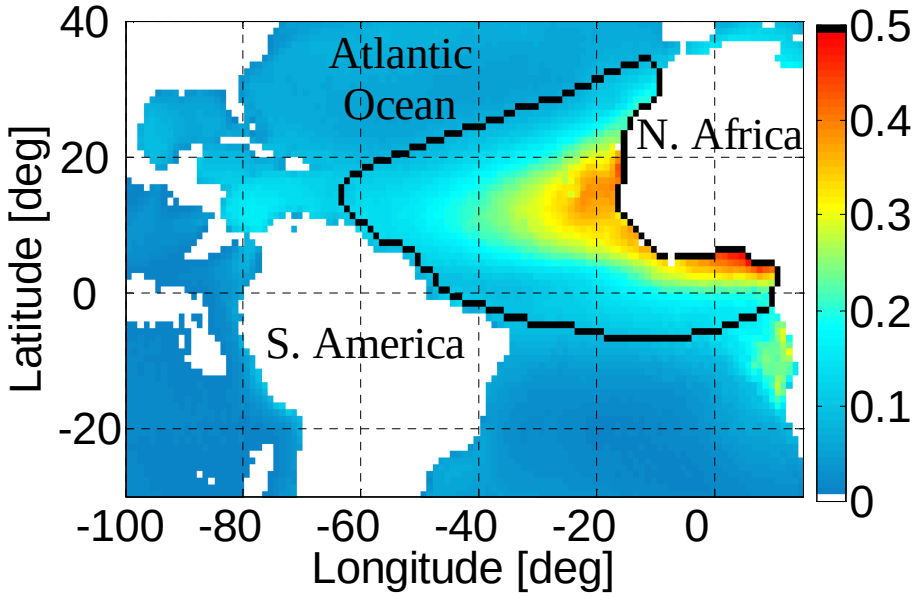

Fig. 1. Averaged values of daily τ_d for the years 2000–2009. The study area is delineated by a black line. Note that high values of τ_d, located outside the study area, near 10° S and 7° E, are most likely attributed by the coarse part of biomass smoke.

ACPD
11, 23513–23539, 2011

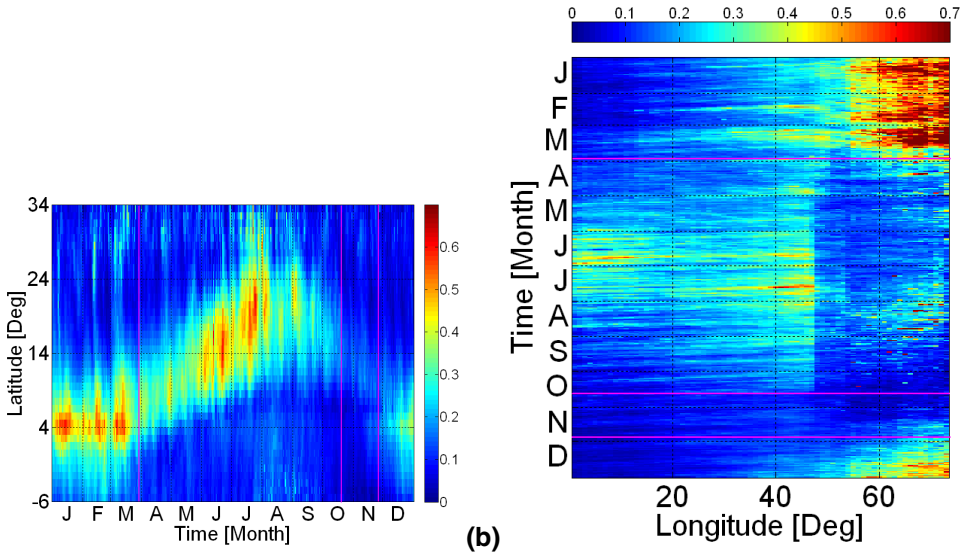

Fig. 2. Hovmöller diagrams of τ_d over the study area. **(a)** Ten year averages of daily τ_d along longitudes. The transitions between the southern-route period, northern-route period and the clean period are marked by magenta line; **(b)** The same as Fig. a, but calculated along latitudes. Note that the apparent line near 16° W is generated due to the shape of the west coast of North Africa (Fig. 1).

ACPD
11, 23513–23539, 2011

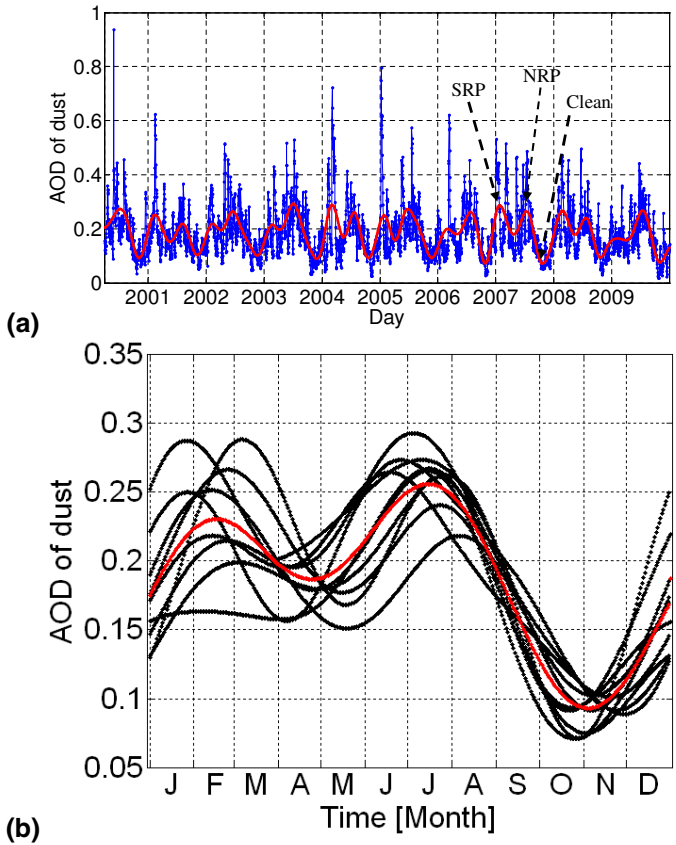

Fig. 3. **(a)** Daily τ_d for the years 2000–2009, averaged over the study area (blue). Smoothed data, generated via the low-pass filter, is shown by the red curve. **(b)** A yearly view of all the smooth data (black) with their average marked in red. The smoothed time series clearly shows a double peak feature for the SRP and NRP, followed by the clean period minimum.

ACPD
11, 23513–23539, 2011




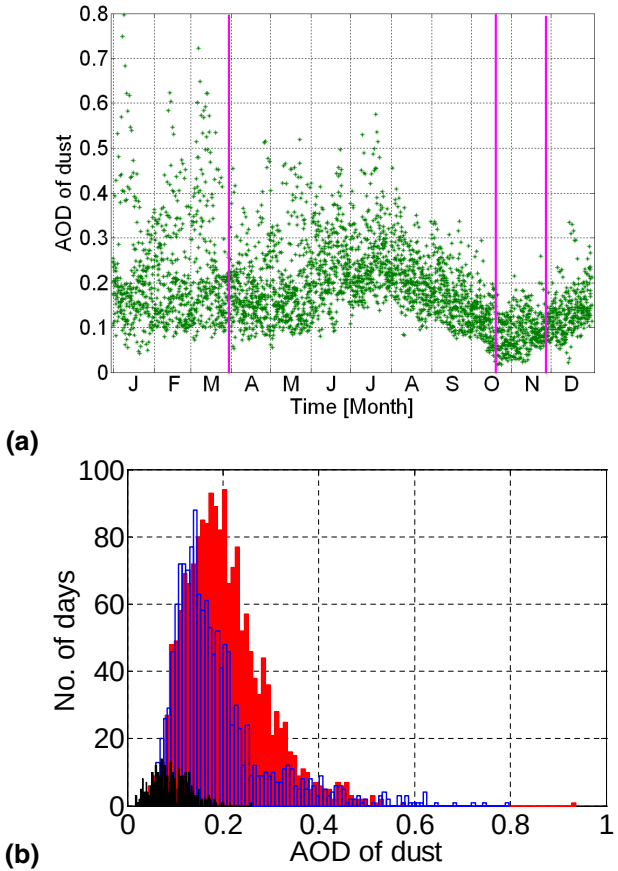

Fig. 4. (a) Daily τ_d averaged over the study area for the years 2000–2009 plotted as a function of time. The transitions between the SRP the NRP and the clean period are marked by magenta lines; **(b)**. Histograms of daily τ_d for the years 2000–2009, averaged over the study area for the NRP (red), SRP (blue) and the clean period (black).

ACPD
11, 23513–23539, 2011

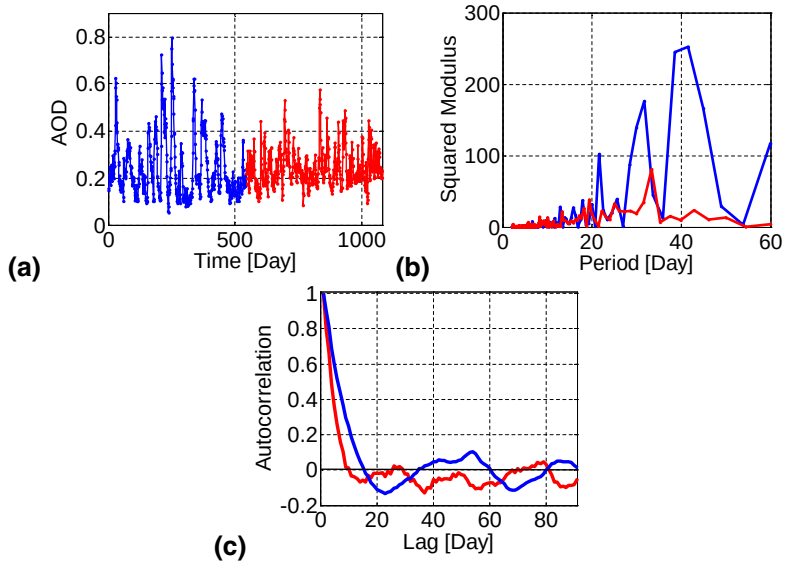

Fig. 5. **(a)** Time series of the SRP (blue) and the NRP (red) signal after subtraction of the seasonality curve. Each signal is composed of 9 segments from 9 years and each segment contains 60 days around the maxima of the period (see red line in Fig. 3), total of 540 points; **(b)** Results of Fourier transform of the two signals in Fig. 5a; **(c)** Autocorrelation analysis for the two periods.

ACPD
11, 23513–23539, 2011

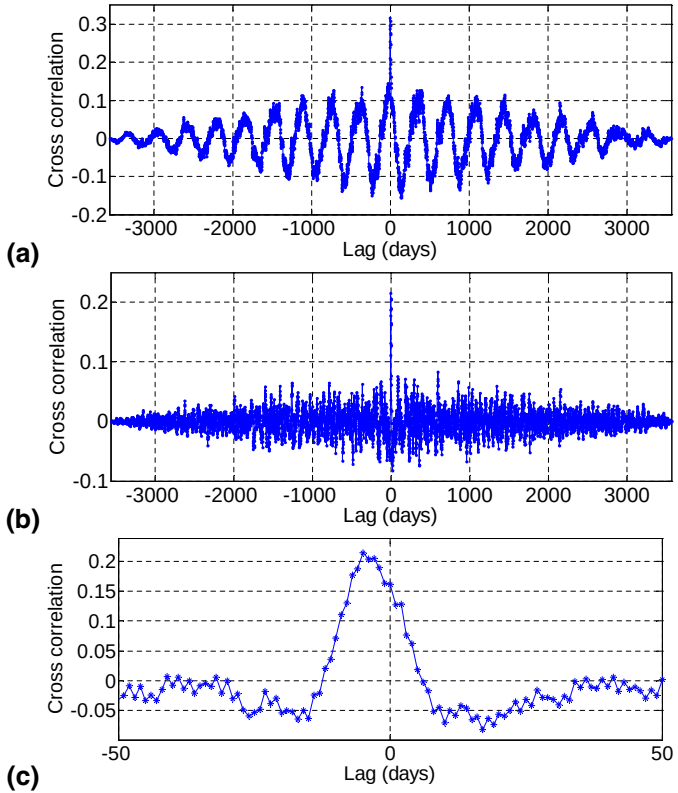

Fig. 6. Cross-correlation between the Bodélé AOD loading (for the area between 18°–15° N and 15°–19° E) and τ_d over the Atlantic Ocean (area marked in Fig. 1) before **(a)**, and after **(b)** subtracting the seasonal signal; **(c)** Enlargement of Fig. b for ±50 days lag.

ACPD
11, 23513–23539, 2011

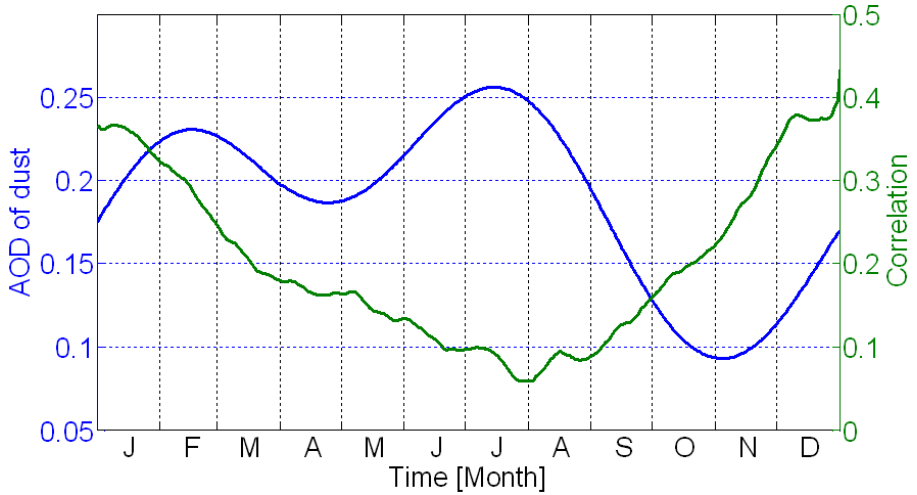

Fig. 7. Three months running correlation analysis between the Bodélé dust loading and the Atlantic AOD signal (green) and the corresponding low pass dust loading over the Atlantic (like in Fig. 3a) in blue.

ACPD
11, 23513–23539, 2011

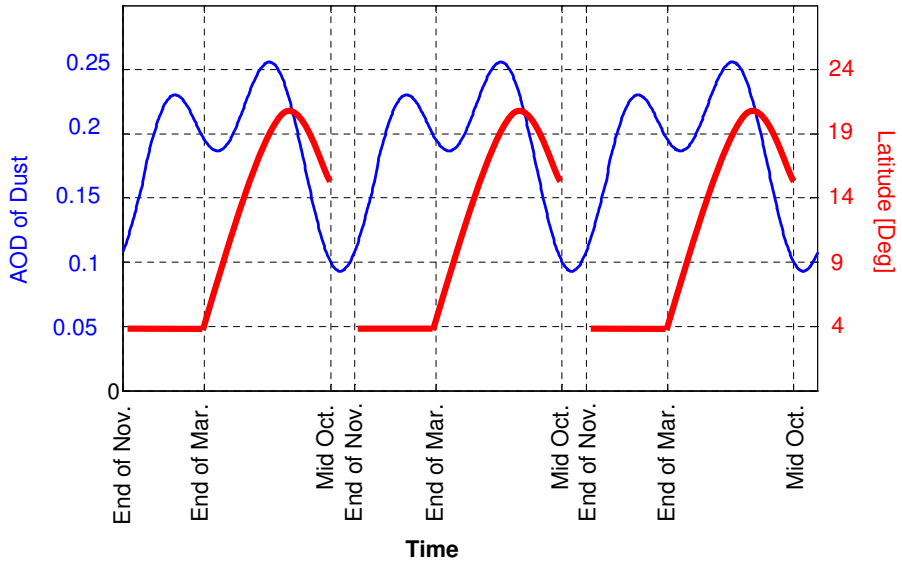

Fig. 8. Schematic illustration of the tri-beat rhythm of the dust loading (in blue) and routes (in red) over the Atlantic.

ACPD
11, 23513–23539, 2011